Positivity-preserving high order methods for the shallow water equations

Yulong Xing

Computer Science and Mathematics Division
Oak Ridge National Laboratory
and Department of Mathematics
University of Tennessee
xingy@math.utk.edu
http://www.math.utk.edu/~xingy/

Joint with Xiangxiong Zhang, Chi-Wang Shu
Brown University

Outline

Shallow water equations with a non-flat bottom topography

$$\begin{cases} h_t + (hu)_x = 0 \\ (hu)_t + \left(hu^2 + \frac{1}{2} g h^2 \right)_x = -ghb_x \end{cases}$$

- h : water height; u : velocity;
  b : bottom topography; g : gravitational constant.

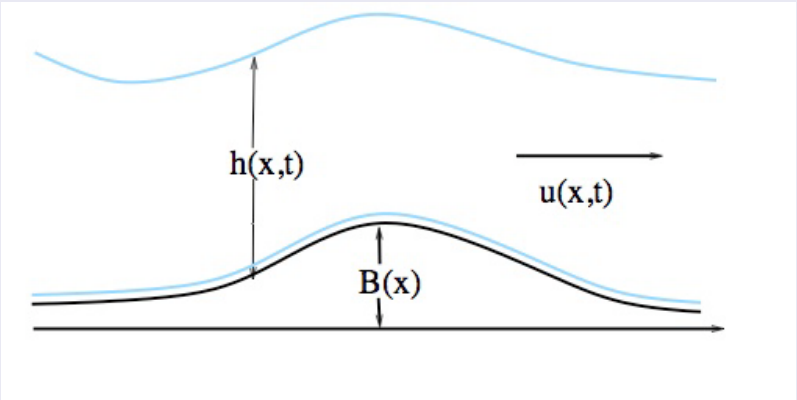

- Other source terms, friction and variations of the channel width, can be added.

Shallow water equations (SWE)

- The SWE are a system of hyperbolic PDEs governing fluid flow in the oceans (sometimes), coastal regions (usually), estuaries (almost always), rivers and channels (almost always).
- The SWE can be used to predict tides, and coastline changes from hurricanes, ocean currents. It also arise in atmospheric flows.
- The SWE are derived from the Navier-Stokes equations, which describe the motion of fluids.
- The general characteristic of shallow water flows is that the vertical dimension is much smaller than the typical horizontal scale. In this case we can average over the depth to get rid of the vertical dimension.

Numerical challenge

- Well-balanced property:
  - Still water at rest steady state:

$$u = 0 \qquad \text{and} \qquad h + b = const.$$

  - Traditional numerical schemes usually fail to capture the steady state well and introduce spurious oscillations. The grid must be extremely refined to reduce the size of these oscillations.
  - Well-balanced methods are developed to reduce the unnecessarily refined mesh. They are specially designed to preserve exactly these steady-state solutions up to machine error with relatively coarse meshes.
  - Several high order well-balanced methods were proposed:
    Xing and Shu 2005, 2006
    Noelle, Pankratz, Puppo and Natvig 2006
    Gallardo, Parés and Castro 2006, 2007
    Caleffi, Valiani and Bernini 2006

Numerical challenge

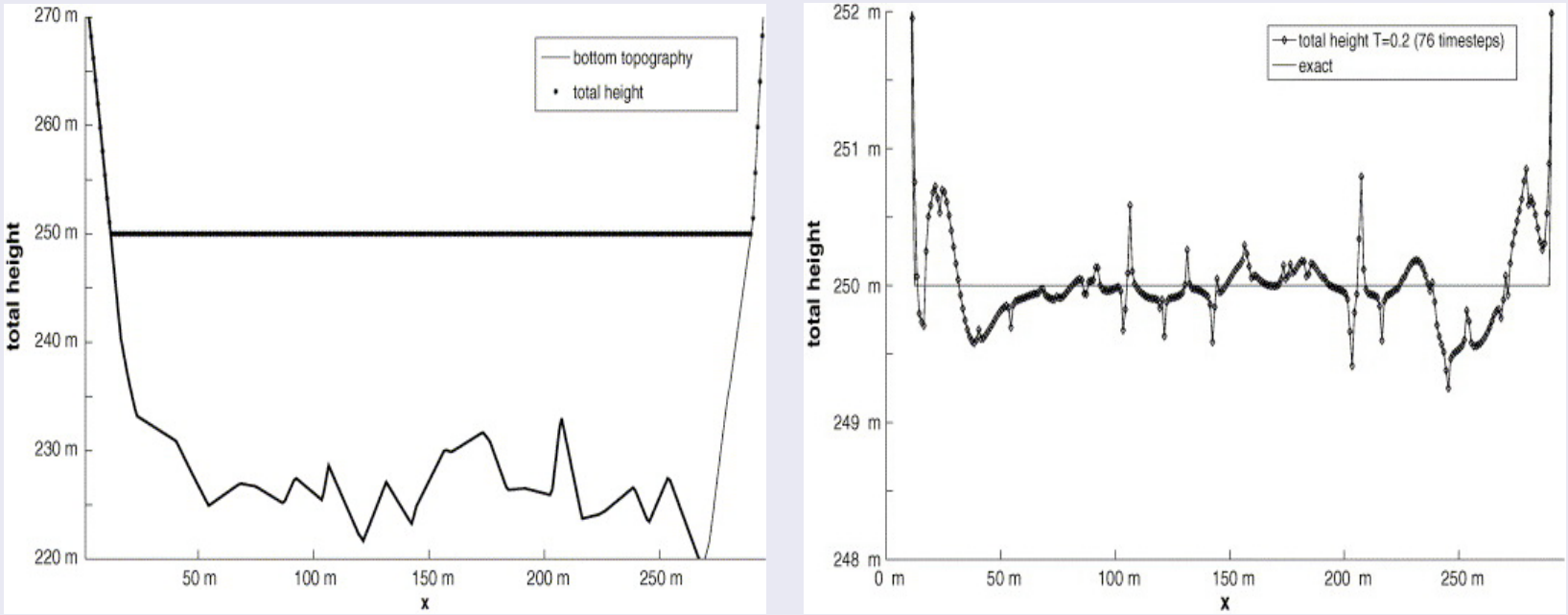

Figure: Numerical computation of Lake Rursee with 296 cells. Left: bottom topography and still water level at time $T = 0$; Right: water level at time $T = 0.2$ (76 time steps) by standard methods. Note: they are copied from Dr. Noelle's Abel Lecture slides with his permission.

Numerical challenge

- Appearance of dry areas:
  - Many applications involve rapidly moving interfaces between wet and dry areas, such as dam breaks, flood waves and run-up phenomena etc.
  - Standard numerical methods may fail near dry/wet front and may produce unacceptable negative water height.
  - Most existing wetting and drying treatments for high order methods focused on post-processing reconstruction of the numerical solution at each time level. It is a challenge to design stable and high order accurate numerical schemes which also have *mass conservation*.

The main objective

Develop positivity-preserving high order accurate well-balanced methods for the shallow water equations, which has the key advantage

- High order accurate
- Well-balanced
- Positivity-preserving without loss of mass conservation
- Good resolution for smooth and discontinuous solutions

Notation

- We denote the mesh by $I_j = [x_{j-\frac{1}{2}}, x_{j+\frac{1}{2}}]$, for $j = 1, \ldots, N$.
- The center of the cell is $x_j = \frac{1}{2}(x_{j-\frac{1}{2}} + x_{j+\frac{1}{2}})$.
- The mesh size is denoted by $\Delta x_j = x_{j+\frac{1}{2}} - x_{j-\frac{1}{2}}$, with $\Delta x = \max_{1 \le j \le N} \Delta x_j$ being the maximum mesh size.
- The piecewise-polynomial space $V_{\Delta x}$ is the space of polynomials of the degree up to k in each cell I_j, i.e.

$$V_{\Delta x} = \{v : \quad v \in P^k(I_j) \quad \text{for } x \in I_j, \quad j = 1, \ldots, N\}.$$

Note that functions in $V_{\Delta x}$ are allowed to have discontinuities across element interfaces.

Discontinuous Galerkin (DG) methods

- Denote the shallow water equations by

$$U_t + f(U)_x = s(h, b)$$

where $U = (h, hu)^T$, $f(U)$ is the flux and $s(h, b)$ is the source term.

- Seek an approximation, still denoted by U with an abuse of notation, which belongs to $V_{\Delta x}$. Similarly, we project b to obtain an approximation, which is denoted by b.

DG methods

$$\int_{I_j} \partial_t U v dx - \int_{I_j} f(U)\partial_x v dx + \widehat{f}_{j+\frac{1}{2}} v(x^-_{j+\frac{1}{2}}) - \widehat{f}_{j-\frac{1}{2}} v(x^+_{j-\frac{1}{2}}) = \int_{I_j} s(h,b) v dx,$$

where $v(x)$ is a test function belonging to $V_{\Delta x}$,

$$\widehat{f}_{j+\frac{1}{2}} = F(U(x^-_{j+\frac{1}{2}}, t), U(x^+_{j+\frac{1}{2}}, t)),$$

and $F(a_1, a_2)$ is a numerical flux. We could, for example, use the simple Lax-Friedrichs flux ($\alpha = \max(|u| + \sqrt{gh})$)

$$F(a_1, a_2) = \frac{1}{2}(f(a_1) + f(a_2) - \alpha(a_2 - a_1)).$$

Forward Euler or total variation diminishing (TVD) high order Runge-Kutta time discretization can be used.

Well-balanced methods

- Preserve the steady state solution

$$u = 0 \qquad \text{and} \qquad h + b = const.$$

  exactly, with only round-off error.
- At the steady state, the first equation $(hu)_x = 0$ is satisfied exactly for any high order scheme.

Well-balanced methods: Approach 1

- Notice the splitting of the source term:

$$-ghb_x = -g(h+b)b_x + \frac{g}{2}b_x^2,$$

and the fact that (when $h+b = const$):

$$\begin{aligned} & D_1\left(\frac{1}{2}gh^2\right) - D_2\left(\frac{1}{2}gb^2\right) + g(h+b)D_3(b) \\ = \quad & D\left(\left(\frac{1}{2}g(h+b)(h-b)\right) + g(h+b)D(b)\right) \\ = \quad & D\left(\frac{1}{2}g(h+b)^2\right) = 0 \end{aligned}$$

if the operators $(D :=)D_1 = D_2 = D_3$ are linear operators.

- Approximate the two derivatives in the source term by the operator used towards the approximation of the flux term.

Well-balanced methods: Approach 2

$$\begin{aligned}\int_{I_j} \partial_t U^n v dx - \int_{I_j} f(U^n)\partial_x v dx &+ \widehat{f}^l_{j+\frac{1}{2}} v(x^-_{j+\frac{1}{2}}) \\ -\widehat{f}^r_{j-\frac{1}{2}} v(x^+_{j-\frac{1}{2}}) &= \int_{I_j} s(h^n, b) v dx,\end{aligned}$$

Reference: Y. Xing and C.-W. Shu, **A new approach of high order well-balanced finite volume WENO schemes and discontinuous Galerkin methods for a class of hyperbolic systems with source terms**, *Communications in Computational Physics*, 1 (2006), pp. 100-134.

Well-balanced fluxes

After computing boundary values $U^{\pm}_{j+\frac{1}{2}}$, we set

$$h^{*,\pm}_{j+\frac{1}{2}} = \max\left(0, h^{\pm}_{j+\frac{1}{2}} + b^{\pm}_{j+\frac{1}{2}} - \max(b^{+}_{j+\frac{1}{2}}, b^{-}_{j+\frac{1}{2}})\right)$$

and redefine the left and right values of U as:

$$U^{*,\pm}_{j+\frac{1}{2}} = \begin{pmatrix} h^{*,\pm}_{j+\frac{1}{2}} \\ h^{*,\pm}_{j+\frac{1}{2}} u^{\pm}_{j+\frac{1}{2}} \end{pmatrix}.$$

Then the left and right fluxes $\widehat{f}^{l}_{j+\frac{1}{2}}$ and $\widehat{f}^{r}_{j-\frac{1}{2}}$ are given by:

$$\begin{aligned} \widehat{f}^{l}_{j+\frac{1}{2}} &= F(U^{*,-}_{j+\frac{1}{2}}, U^{*,+}_{j+\frac{1}{2}}) + \begin{pmatrix} 0 \\ \frac{g}{2}(h^{-}_{j+\frac{1}{2}})^2 - \frac{g}{2}(h^{*,-}_{j+\frac{1}{2}})^2 \end{pmatrix} \\ \widehat{f}^{r}_{j-\frac{1}{2}} &= F(U^{*,-}_{j-\frac{1}{2}}, U^{*,+}_{j-\frac{1}{2}}) + \begin{pmatrix} 0 \\ \frac{g}{2}(h^{+}_{j-\frac{1}{2}})^2 - \frac{g}{2}(h^{*,+}_{j-\frac{1}{2}})^2 \end{pmatrix}. \end{aligned}$$

Well-balanced properties

At the steady state $h + b = const$, $hu = 0$, we have

$$\hat{f}^l_{j+\frac{1}{2}} = f(U^n(x^-_{j+\frac{1}{2}}, t)), \qquad \hat{f}^r_{j-\frac{1}{2}} = f(U^n(x^+_{j-\frac{1}{2}}, t)).$$

Then the residue R becomes:

$$\begin{aligned}
R &= -\int_{I_j} f(U^n)\partial_x v dx + \hat{f}^l_{j+\frac{1}{2}} v(x^-_{j+\frac{1}{2}}) - \hat{f}^r_{j-\frac{1}{2}} v(x^+_{j-\frac{1}{2}}) - \int_{I_j} s(h^n, b) v dx \\
&= -\int_{I_j} f(U^n)\partial_x v dx + f(U^n(x^-_{j+\frac{1}{2}}, t)) v(x^-_{j+\frac{1}{2}}) \\
&\quad -f(U^n(x^+_{j-\frac{1}{2}}, t)) v(x^+_{j-\frac{1}{2}}) - \int_{I_j} s(h^n, b) v dx \\
&= \int_{I_j} \partial_x f(U^n) v dx - \int_{I_j} s(h^n, b) v dx \\
&= \int_{I_j} (\partial_x f(U^n) - s(h^n, b)) v dx = 0.
\end{aligned}$$

Weighted essentially non-oscillatory (WENO) methods

$\bar{U}_j(t)$ approximates the cell averages $\frac{1}{\Delta x_j}\int_{I_j} U(x,t)\,dx$, and satisfies

$$\frac{d}{dt}\bar{U}_j(t) + \frac{1}{\Delta x_j}\left(\hat{f}_{j+\frac{1}{2}} - \hat{f}_{j-\frac{1}{2}}\right) = \frac{1}{\Delta x_j}\int_{I_j} s(h,b)dx,$$

where

$$\hat{f}_{j+\frac{1}{2}} = F(U^-_{j+\frac{1}{2}}, U^+_{j+\frac{1}{2}}).$$

$U^-_{j+\frac{1}{2}}$ and $U^+_{j+\frac{1}{2}}$, the high order pointwise approximations to $U(x_{j+\frac{1}{2}}, t)$ from left and right respectively, are computed through the neighboring cell average values $\bar{U}_j$ by a high order WENO reconstruction procedure.

Well-balanced WENO methods

$$\frac{d}{dt}\bar{U}_j(t) + \frac{1}{\Delta x_j}\left(\hat{f}^l_{j+\frac{1}{2}} - \hat{f}^r_{j-\frac{1}{2}}\right) = \frac{1}{\Delta x_j}\int_{I_j} s(h^n, b)dx.$$

To compute $\int_{I_j} s(h, b)dx$, we use interpolation to obtain a high order polynomial h_h (or b_h) on the cell I_j, based on the reconstructed boundary values, and compute $\int_{I_j} s(h_h, b_h)dx$ exactly by a suitable Gauss quadrature.

Main result

Proposition: Consider the scheme satisfied by the cell averages of the water height in the well-balanced DG/WENO method. If $h^-_{j-\frac{1}{2}}$, $h^+_{j+\frac{1}{2}}$ and $h^n_j(x)$ are all non-negative, then $\overline{h}^{n+1}_j$ is also non-negative under the CFL condition

$$\lambda\alpha \leq \widehat{w}_1.$$

Cell averages

Consider the cell averages in the well-balanced DG/WENO methods, with a simple Euler forward time discretization.

The cell averages of the height satisfy

$$\overline{h}_j^{n+1} = \overline{h}_j^n - \lambda \left[\widehat{F}\left(h^{*,-}_{j+\frac{1}{2}}, u^-_{j+\frac{1}{2}}; h^{*,+}_{j+\frac{1}{2}}, u^+_{j+\frac{1}{2}} \right) - \widehat{F}\left(h^{*,-}_{j-\frac{1}{2}}, u^-_{j-\frac{1}{2}}; h^{*,+}_{j-\frac{1}{2}}, u^+_{j-\frac{1}{2}} \right) \right],$$

where

$$\begin{aligned} & \widehat{F}\left(h^{*,-}_{j+\frac{1}{2}}, u^-_{j+\frac{1}{2}}; h^{*,+}_{j+\frac{1}{2}}, u^+_{j+\frac{1}{2}} \right) \\ = & \frac{1}{2}\left(h^{*,-}_{j+\frac{1}{2}} u^-_{j+\frac{1}{2}} + h^{*,+}_{j+\frac{1}{2}} u^+_{j+\frac{1}{2}} - \alpha(h^{*,+}_{j+\frac{1}{2}} - h^{*,-}_{j+\frac{1}{2}}) \right). \end{aligned}$$

First order scheme with the well-balanced flux

Lemma 3.1: Under the CFL condition $\lambda\alpha \leq 1$, with $\alpha = \max(|u| + \sqrt{gh})$, consider the following scheme

$$\begin{aligned} h_j^{n+1} &= h_j^n - \lambda\left[\widehat{F}\left(h_j^{*,+}, u_j^n; h_{j+1}^{*,-}, u_{j+1}^n\right) - \widehat{F}\left(h_{j-1}^{*,+}, u_{j-1}^n; h_j^{*,-}, u_j^n\right)\right] \\ h_j^{*,+} &= \max\left(0, h_j^n + b_j - \max(b_j, b_{j+1})\right) \\ h_j^{*,-} &= \max\left(0, h_j^n + b_j - \max(b_{j-1}, b_j)\right). \end{aligned}$$

If h_j^n, $h_{j\pm1}^n$ are non-negative, then h_j^{n+1} is also non-negative.

Proof:

$$\begin{aligned} h_j^{n+1} = &\left[1 - \frac{1}{2}\lambda\left(\alpha + u_j^n\right)\frac{h_j^{*,-}}{h_j^n} - \frac{1}{2}\lambda\left(\alpha - u_j^n\right)\frac{h_j^{*,+}}{h_j^n}\right] h_j^n \\ &+ \left[\frac{1}{2}\lambda\left(\alpha + u_{j-1}^n\right)\frac{h_{j-1}^{*,+}}{h_{j-1}^n}\right] h_{j-1}^n + \left[\frac{1}{2}\lambda\left(\alpha - u_{j+1}^n\right)\frac{h_{j+1}^{*,-}}{h_{j+1}^n}\right] h_{j+1}^n. \end{aligned}$$

Gauss-Lobatto quadrature

N-points Legendre Gauss-Lobatto quadrature points on I_j:

$$S_j = \left\{ x_{j-\frac{1}{2}} = \widehat{x}_j^1, \widehat{x}_j^2, \cdots, \widehat{x}_j^{N-1}, \widehat{x}_j^N = x_{j+\frac{1}{2}} \right\},$$

exact for the integral of polynomials of degree up to $2N-3 \geq k$. $\widehat{w}_t$ be the quadrature weights for the interval $[-1/2, 1/2]$.

We have

$$\overline{h}_j^n = \frac{1}{\Delta x} \int_{I_j} h_j^n(x) dx = \sum_{t=1}^{N} \widehat{w}_t h_j^n(\widehat{x}_j^t) = \sum_{t=2}^{N-1} \widehat{w}_t h_j^n(\widehat{x}_j^t) + \widehat{w}_1 h_{j-\frac{1}{2}}^+ + \widehat{w}_N h_{j+\frac{1}{2}}^-$$

since the quadrature is exact for polynomials of degree k.

Main result

Proposition 3.2: Consider the scheme satisfied by the cell averages of the water height in the well-balanced DG/WENO method. If $h^-_{j-\frac{1}{2}}$, $h^+_{j+\frac{1}{2}}$ and $h^n_j(x)$ are all non-negative, then $\overline{h}^{n+1}_j$ is also non-negative under the CFL condition

$$\lambda\alpha \leq \widehat{w}_1.$$

Main result

Proof:

$$\begin{aligned}
\overline{h}_j^{n+1} &= \sum_{t=2}^{N-1} \widehat{w}_t h_j^n(\widehat{x}_j^t) + \widehat{w}_1 h^+_{j-\frac{1}{2}} + \widehat{w}_N h^-_{j+\frac{1}{2}} \\
&\quad -\lambda \left[\widehat{F}\left(h^{*,-}_{j+\frac{1}{2}}, u^-_{j+\frac{1}{2}}; h^{*,+}_{j+\frac{1}{2}}, u^+_{j+\frac{1}{2}}\right) - \widehat{F}\left(h^{*,+}_{j-\frac{1}{2}}, u^+_{j-\frac{1}{2}}; h^{*,-}_{j+\frac{1}{2}}, u^-_{j+\frac{1}{2}}\right) \right. \\
&\quad \left. + \widehat{F}\left(h^{*,+}_{j-\frac{1}{2}}, u^+_{j-\frac{1}{2}}; h^{*,-}_{j+\frac{1}{2}}, u^-_{j+\frac{1}{2}}\right) - \widehat{F}\left(h^{*,-}_{j-\frac{1}{2}}, u^-_{j-\frac{1}{2}}; h^{*,+}_{j-\frac{1}{2}}, u^+_{j-\frac{1}{2}}\right) \right] \\
&= \sum_{t=2}^{N-1} \widehat{w}_t h_j^n(\widehat{x}_j^t) + \widehat{w}_N H_N + \widehat{w}_1 H_1,
\end{aligned}$$

where

$$H_1 = h^+_{j-\frac{1}{2}} - \frac{\lambda}{\widehat{w}_1}\left[\widehat{F}\left(h^{*,+}_{j-\frac{1}{2}}, u^+_{j-\frac{1}{2}}; h^{*,-}_{j+\frac{1}{2}}, u^-_{j+\frac{1}{2}}\right) - \widehat{F}\left(h^{*,-}_{j-\frac{1}{2}}, u^-_{j-\frac{1}{2}}; h^{*,+}_{j-\frac{1}{2}}, u^+_{j-\frac{1}{2}}\right)\right]$$

$$H_N = h^-_{j+\frac{1}{2}} - \frac{\lambda}{\widehat{w}_N}\left[\widehat{F}\left(h^{*,-}_{j+\frac{1}{2}}, u^-_{j+\frac{1}{2}}; h^{*,+}_{j+\frac{1}{2}}, u^+_{j+\frac{1}{2}}\right) - \widehat{F}\left(h^{*,+}_{j-\frac{1}{2}}, u^+_{j-\frac{1}{2}}; h^{*,-}_{j+\frac{1}{2}}, u^-_{j+\frac{1}{2}}\right)\right].$$

Positivity-preserving limiter

To enforce the conditions of this proposition, we introduce the following limiter on the DG polynomial $U_j^n(x) = (h_j^n(x), (hu)_j^n(x))^T$,

$$\widetilde{U}_j^n(x) = \theta\left(U_j^n(x) - \overline{U}_j^n\right) + \overline{U}_j^n, \qquad \theta = \min\left\{1, \frac{\overline{h}_j^n}{\overline{h}_j^n - m_j}\right\},$$

with

$$m_j = \min_{x \in I_j} h_j^n(x).$$

and use this $\widetilde{U}_j^n(x)$ to compute the numerical flux.

Easy to observe that $\widetilde{h}_j^n(x) \geq 0$.

Properties of this limiter

- Keeps water height non-negative;
- Preserves the local conservation of h and hu;
- Does not destroy the high order accuracy;
- Only active in the dry or nearly dry region.

Implementation of this limiter

We need to evaluate the minimum of a polynomial in

$$m_j = \min_{x \in I_j} h_j^n(x), \tag{1}$$

which can be difficult in the 2D case.

In the implementation, we replace it by:

$$m_j = \min(h^+_{j-\frac{1}{2}}, h^-_{j+\frac{1}{2}}, \xi_j), \tag{2}$$

where

$$\xi_j = \frac{1}{\sum_{r=2}^{N-1} \hat{w}_r} \sum_{t=2}^{N-1} \hat{w}_r p_j(\hat{x}_j^r) = \frac{\overline{h}_j^n - \hat{w}_1 h^+_{j-\frac{1}{2}} - \hat{w}_N h^-_{j+\frac{1}{2}}}{1 - \hat{w}_1 - \hat{w}_N}.$$

It can be proven that this simplified limiter (2) inherits the desirable properties of the original limiter (1).

Comments

- Works for TVD high order Runge-Kutta and multi-step time discretizations.
- Positivity preserving CFL condition is $\lambda\alpha \leq 1/6$ for $k = 2, 3$. Recall that the CFL condition for linear stability for the DG methods is $\lambda\alpha \leq 1/5$ for $k = 2$.
- Any other positivity-preserving exact or approximate Rieman solver, including Godunov, Boltzmann type and Harten-Lax-Van Leer, can also be used.
- Works for non-well-balanced DG/WENO methods.

Table: The CFL condition for $2 \leq k \leq 5$ and the Gauss-Lobatto quadrature points on $[-\frac{1}{2}, \frac{1}{2}]$.

k	CFL	quadrature points on $[-\frac{1}{2}, \frac{1}{2}]$
2	$\lambda\alpha \leq \frac{1}{6}$	$\{-\frac{1}{2}, 0, \frac{1}{2}\}$
3	$\lambda\alpha \leq \frac{1}{6}$	$\{-\frac{1}{2}, 0, \frac{1}{2}\}$
4	$\lambda\alpha \leq \frac{1}{12}$	$\{-\frac{1}{2}, -\frac{1}{\sqrt{20}}, \frac{1}{\sqrt{20}}, \frac{1}{2}\}$
5	$\lambda\alpha \leq \frac{1}{12}$	$\{-\frac{1}{2}, -\frac{1}{\sqrt{20}}, \frac{1}{\sqrt{20}}, \frac{1}{2}\}$

Algorithm flowchart

- Evaluate m_j.
- Use the positivity-preserving limiter to compute $\widetilde{U}_j^n(x)$.
- Compute the well-balanced fluxes from $\widetilde{U}_j^n(x)$.
- Use $\widetilde{U}_j^n(x)$ instead of $U_j^n(x)$ in the scheme with the corresponding CFL condition.

Two-dimensional shallow water system

$$\begin{cases} h_t + (hu)_x + (hv)_y = 0 \\ (hu)_t + \left(hu^2 + \frac{1}{2}gh^2\right)_x + (huv)_y = -ghb_x \\ (hv)_t + (huv)_x + \left(hv^2 + \frac{1}{2}gh^2\right)_y = -ghb_y. \end{cases}$$

- Still water at rest steady state:

$$h + b = const, \qquad hu = 0, \qquad hv = 0.$$

- Consider rectangular meshes.

Quadrature points

- N-points Gauss-Lobatto quadrature points

$$\begin{aligned} \widehat{S}_i^x &= \{\widehat{x}_i^t : t = 1, \cdots, N\} \\ \widehat{S}_j^y &= \{\widehat{y}_j^t : t = 1, \cdots, N\} \end{aligned}$$

on $[x_{i-\frac{1}{2}}, x_{i+\frac{1}{2}}]$ and $[y_{j-\frac{1}{2}}, y_{j+\frac{1}{2}}]$, respectively.

- L-points Gauss quadrature points

$$\begin{aligned} S_i^x &= \{x_i^\beta : \beta = 1, \cdots, L\} \\ S_j^y &= \{y_j^\beta : \beta = 1, \cdots, L\} \end{aligned}$$

to compute the integrals.

Main result

Proposition: Consider the well-balanced DG scheme solving the 2D shallow water equations. If $h_{i,j}^n(x,y) \geq 0$ for all the i,j, then $\overline{h}_{i,j}^{n+1} \geq 0$ under the CFL condition

$$\frac{\Delta t}{\Delta x} \parallel (|u| + \sqrt{gh}) \parallel_\infty + \frac{\Delta t}{\Delta y} \parallel (|v| + \sqrt{gh}) \parallel_\infty \leq \widehat{w}_1.$$

Positivity preserving limiter

$$\widetilde{U}_{ij}^n(x,y) = \theta\left(U_{ij}^n(x,y) - \overline{U}_{ij}^n\right) + \overline{U}_{ij}^n, \qquad \theta = \min\left\{1, \frac{\overline{h}_{ij}^n}{\overline{h}_{ij}^n - m_{i,j}}\right\},$$

where

$$m_{i,j} = \min_{(x,y)\in I_{ij}} h_{ij}^n(x,y).$$

In the implementation, we replace it by

$$m_{i,j} = \min(h_{ij}^{\pm}(x_i^\beta, y_{j\mp\frac{1}{2}}), h_{ij}^{\pm}(x_{i\mp\frac{1}{2}}, y_j^\beta), \xi_{i,j}^1, \xi_{i,j}^2),$$

where

$$\xi_{i,j}^1 = \frac{\overline{h}_{i,j}^n - \widehat{w}_1 \sum_{\beta=1}^L w_\beta h_{i,j}^n(x_i^\beta, y_{j-\frac{1}{2}}) - \widehat{w}_N \sum_{\beta=1}^L w_\beta h_{i,j}^n(x_i^\beta, y_{j+\frac{1}{2}})}{1 - \widehat{w}_1 - \widehat{w}_N},$$

$$\xi_{i,j}^2 = \frac{\overline{h}_{i,j}^n - \widehat{w}_1 \sum_{\beta=1}^L w_\beta h_{i,j}^n(x_{i-\frac{1}{2}}, y_j^\beta) - \widehat{w}_N \sum_{\beta=1}^L w_\beta h_{i,j}^n(x_{i+\frac{1}{2}}, y_j^\beta)}{1 - \widehat{w}_1 - \widehat{w}_N}.$$

Numerical methods

- The third order finite element DG methods (i.e. $k = 2$), coupled with the third order TVD Runge-Kutta time discretization are implemented.
- The CFL number is taken as 0.16.
- The gravitation constant g is fixed as $9.812\, m/s^2$.

Tests for well-balanced property

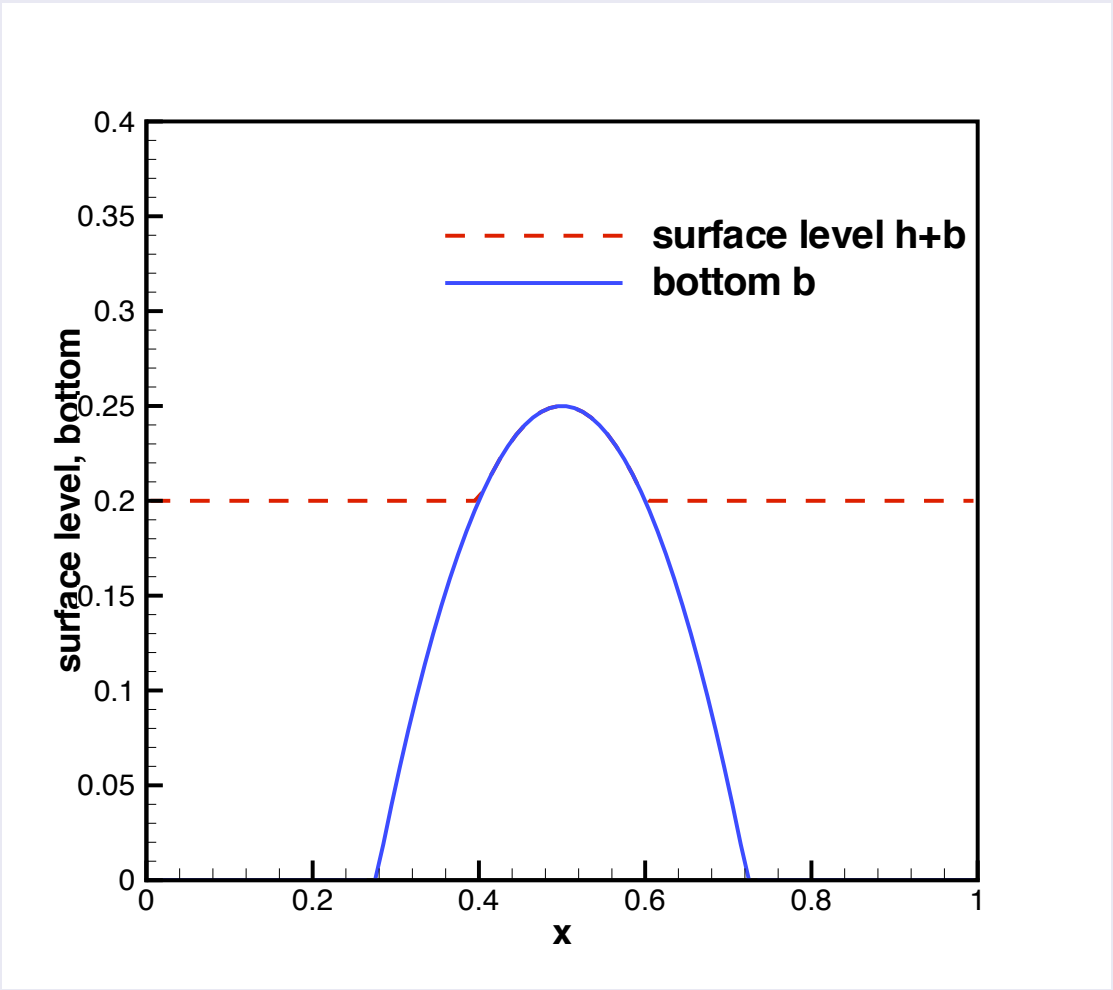

Figure: The surface level $h + b$ and the bottom b for the stationary flow.

Tests for well-balanced property

Table: L^1 and L^∞ errors for different precisions for the stationary solution.

precision	L^1 error		L^∞ error	
	h	hu	h	hu
single	2.89E-07	1.14E-07	5.81E-07	4.20E-07
double	7.16E-16	1.94E-16	1.11E-15	1.42E-15

Accuracy test

- Initial conditions

$$\begin{aligned} h(x,0) &= 5 + e^{\cos(2\pi x)}, \qquad (hu)(x,0) = \sin(\cos(2\pi x)), \\ b(x) &= \sin^2(\pi x), \qquad \text{for } x \in [0,1], \end{aligned}$$

  with periodic boundary conditions.

- Use $N = 12,800$ cells to compute a reference solution, and treat this as the exact solution in computing the numerical errors.
- The TVB constant M in the limiter is taken as 32. We compute up to $t = 0.1$.

Accuracy test

Table: L^1 errors and numerical orders of accuracy for the example.

No. of cells	h		hu	
	L^1 error	order	L^1 error	order
25	2.12E-03		1.83E-02	
50	1.10E-04	4.27	9.73E-04	4.23
100	1.15E-05	3.26	1.02E-04	3.25
200	8.79E-07	3.72	7.72E-06	3.72
400	9.38E-08	3.23	8.26E-07	3.22
800	1.07E-08	3.13	9.41E-08	3.13

Riemann problem over a flat bottom

Consider two Riemann problems over a flat bottom

- Test case 1: in [-300, 300]

$$hu(x,0) = 0 \quad \text{and} \quad h(x,0) = \begin{cases} 10 & \text{if } x \leq 0, \\ 0 & \text{otherwise.} \end{cases}$$

- Test case 2: in [-200, 400]

$$h(x,0) = \begin{cases} 5 & \text{if } x \leq 0, \\ 10 & \text{otherwise,} \end{cases} \quad \text{and} \quad u(x,0) = \begin{cases} 0 & \text{if } x \leq 0, \\ 40 & \text{otherwise.} \end{cases}$$

Riemann problem: Test case 1

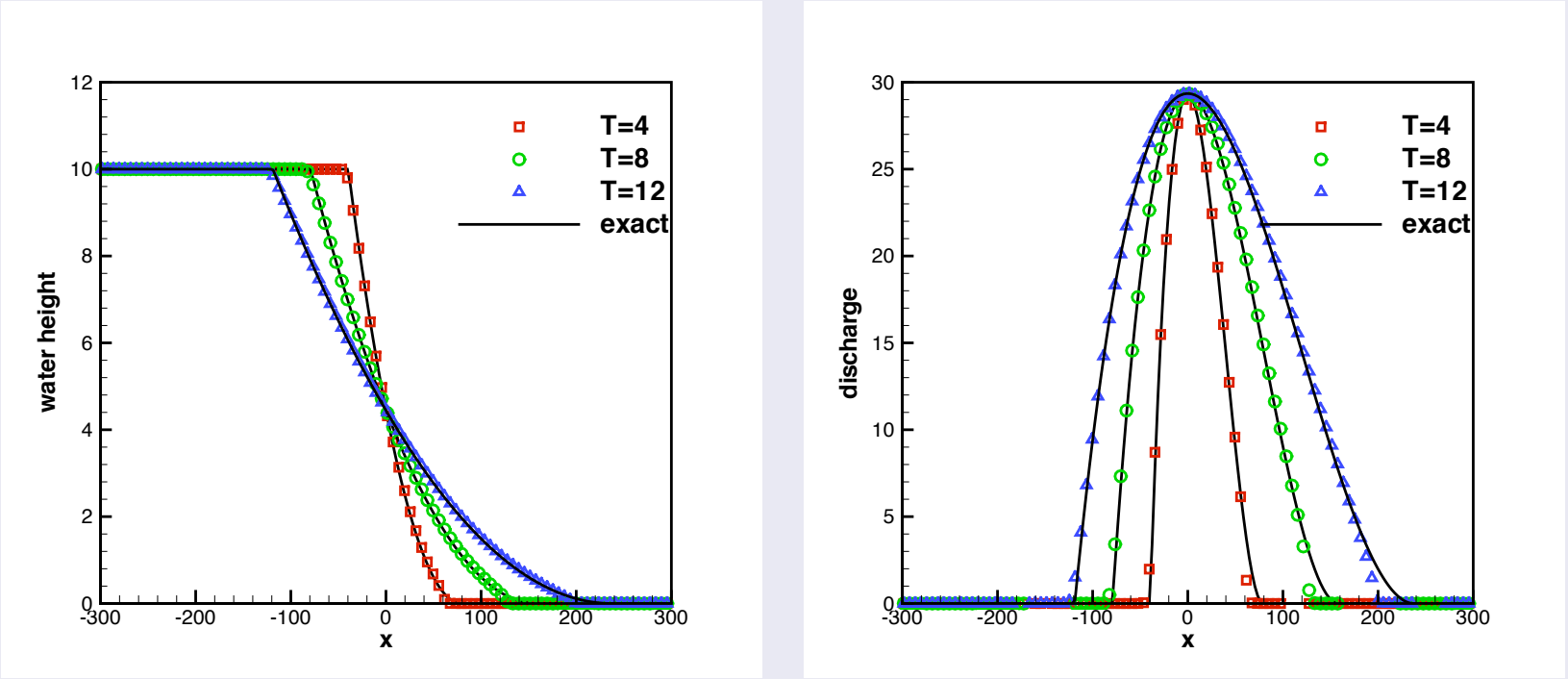

Figure: The numerical and exact solutions of the first Riemann problem at different time with 200 uniform cells. Left: the water height h; Right: the discharge hu.

Riemann problem: Test case 1

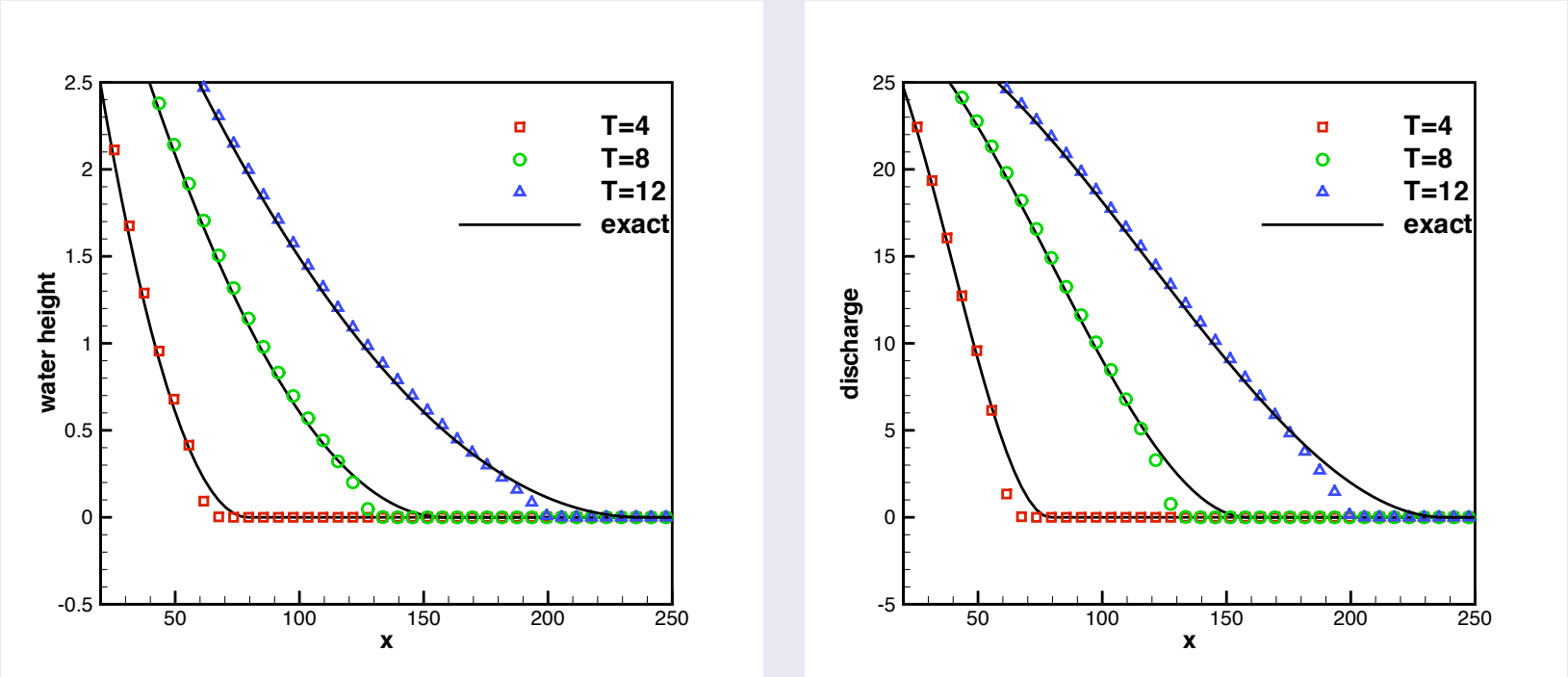

Figure: Zoom-in of the wet/dry front.

Riemann problem: Test case 2

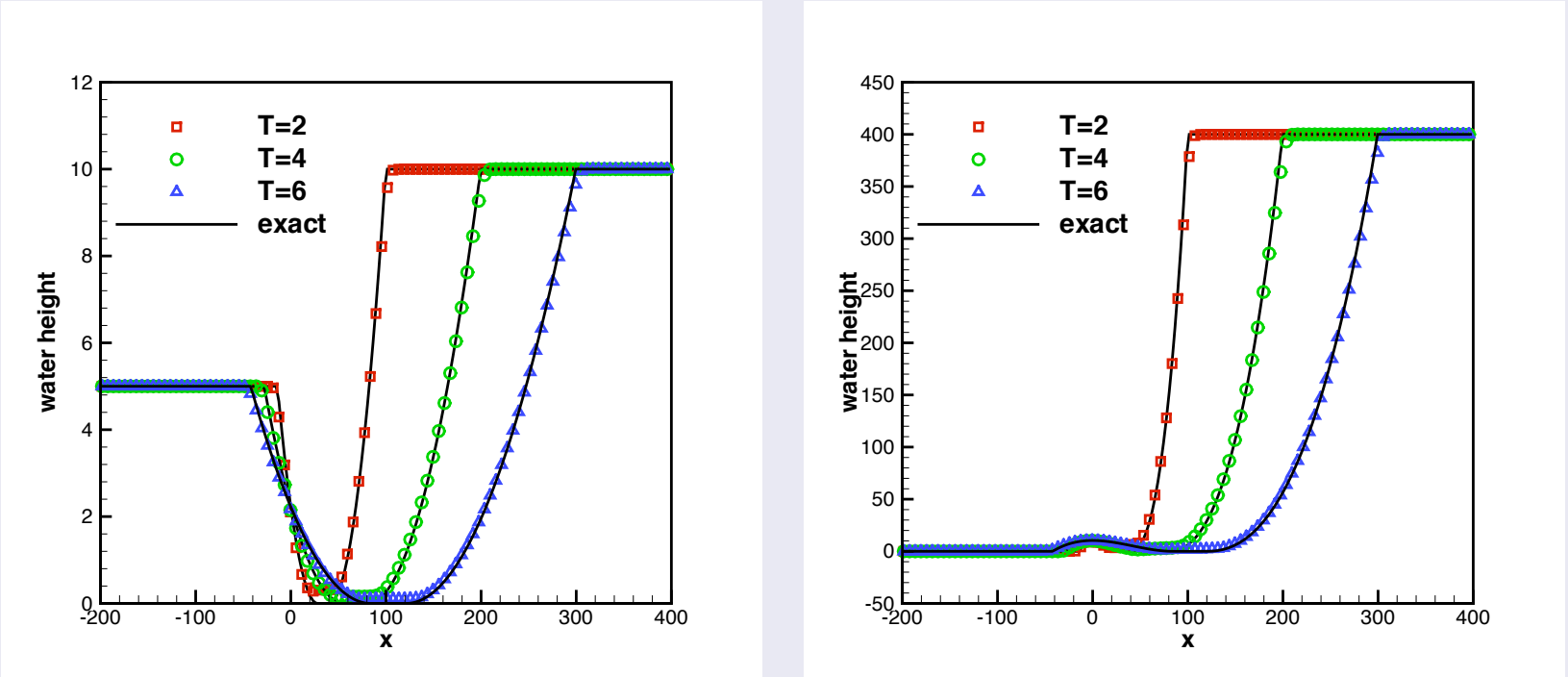

Figure: The numerical and exact solutions of the second Riemann problem at different time with 300 uniform cells. Left: the water height h; Right: the discharge hu.

Riemann problem: Test case 2

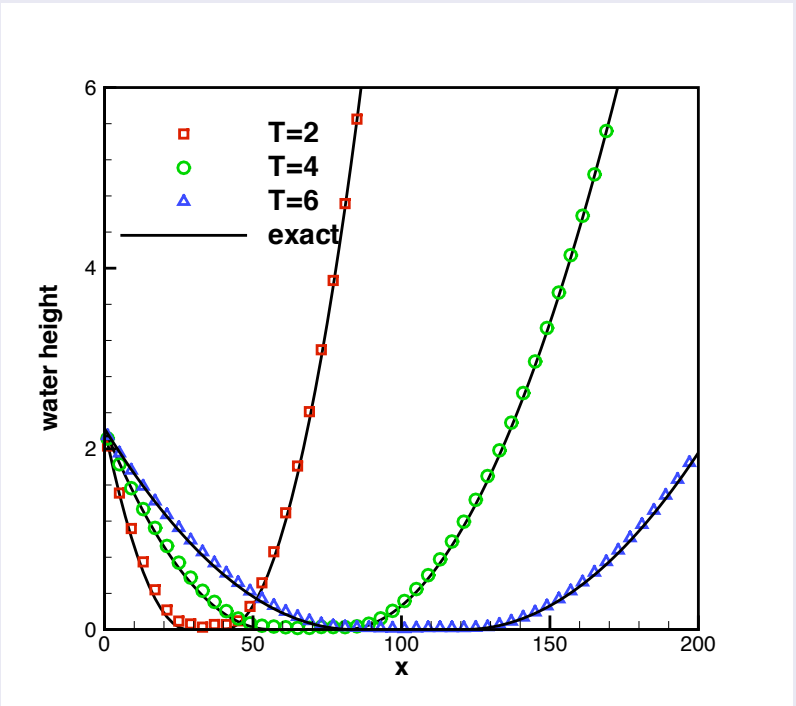

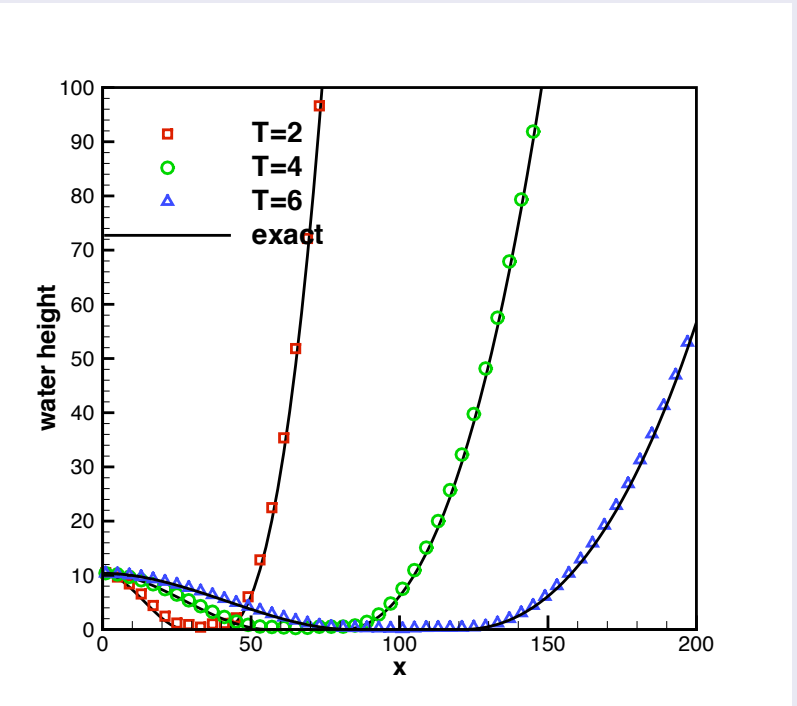

Figure: , zoom-in of the wet/dry front.

Dam break over a plane

- Computational domain [-15, 15] and initial conditions:

$$\begin{aligned} hu(x,0) &= 0, \quad h(x,0) = \begin{cases} 1 - b(x) & \text{if } x \leq 0, \\ 0 & \text{otherwise,} \end{cases} \\ b(x) &= 1 - x\tan(\alpha), \end{aligned}$$

  with some angle α which will be defined later.

- The discharge $q = 0$ is imposed at the left boundary $x = -15$ and a free boundary condition is considered at the right boundary $x = 15$.

Dam break over a plane

- Exact position of the wet/dry front and its velocity

$$\begin{aligned} x_f(t) &= 2t\sqrt{g\cos(\alpha)} - \frac{1}{2}gt^2\tan(\alpha), \\ u_f(t) &= 2\sqrt{g\cos(\alpha)} - gt\tan(\alpha), \end{aligned}$$

- Three different values of α considered:
  1. emerging topography $\alpha = \pi/60$,
  2. the flat bottom $\alpha = 0$
  3. bottom with decreasing depth $\alpha = -\pi/60$.
- Stopping time $t = 2$, with 300 uniform cells.

Dam break over a plane

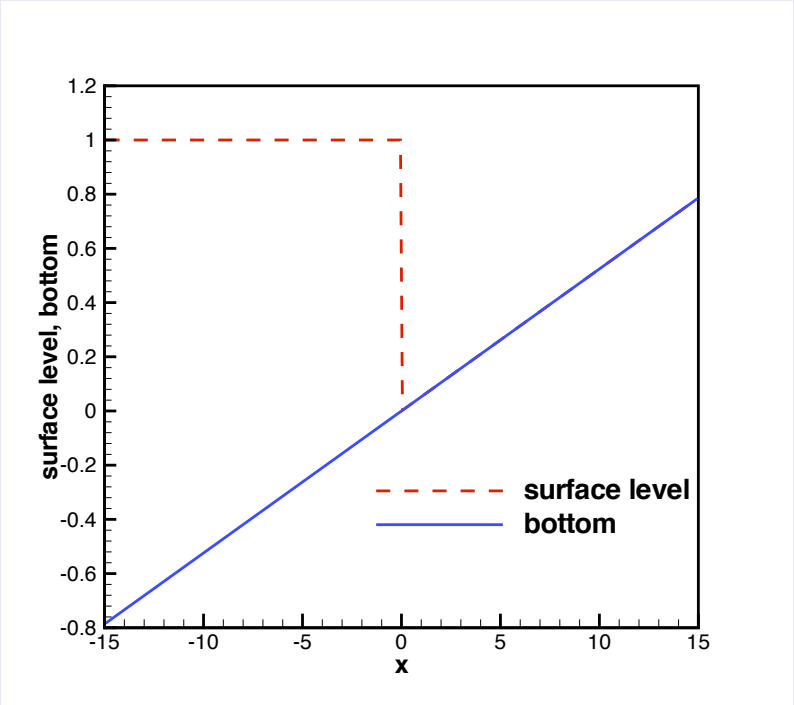

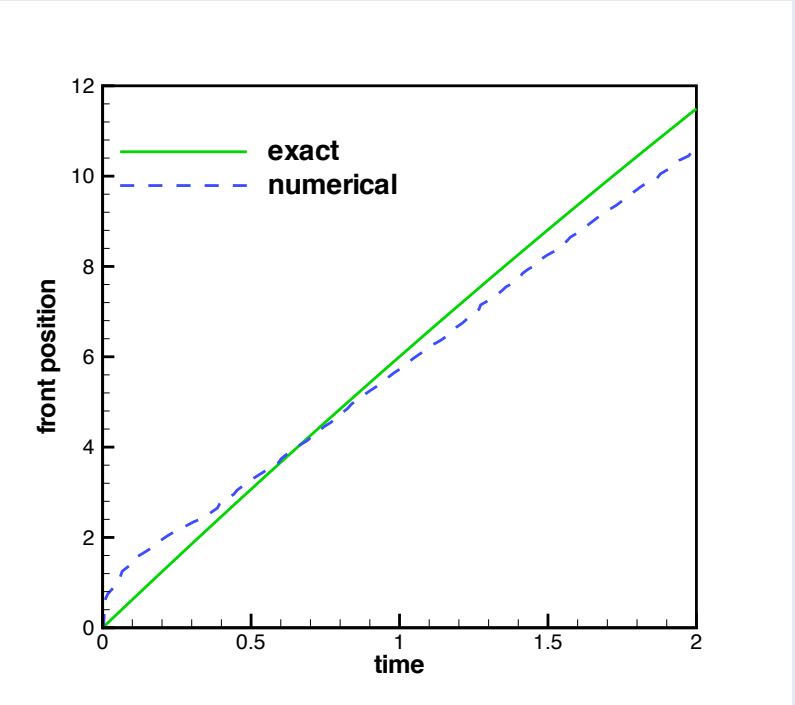

Figure: The numerical results of the dambreak problem over an emerging topography with $\alpha = \pi/60$. Left: the initial condition; Right: time evolution of wet/dry front location.

Dam break over a plane

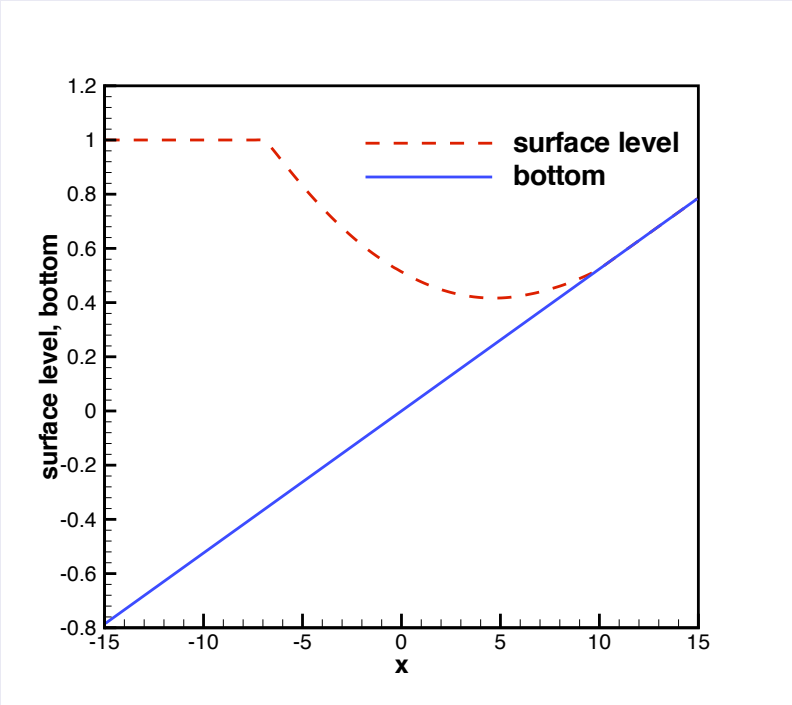

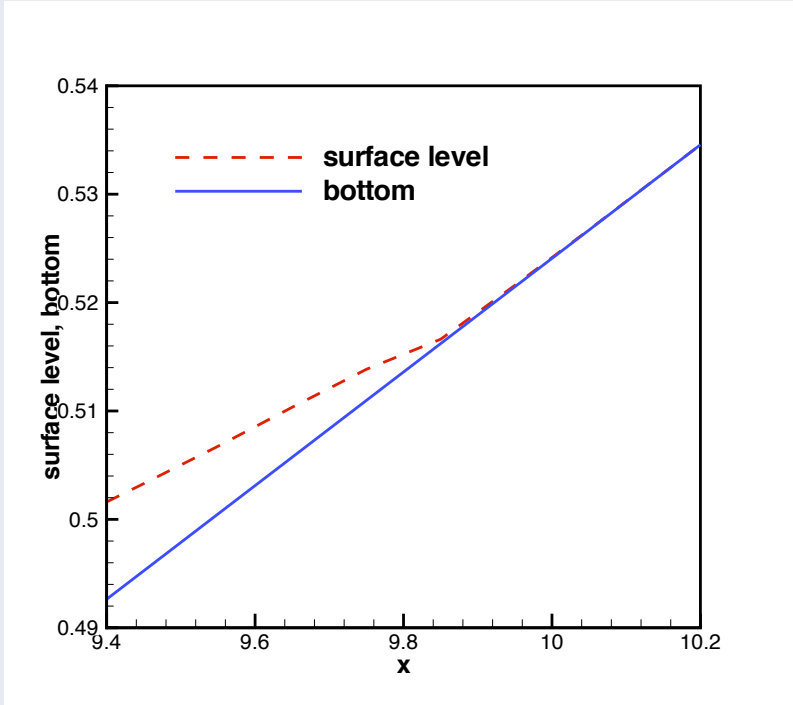

Figure: The numerical results of the dambreak problem over an emerging topography with $\alpha = \pi/60$. Left: surface level at time $t = 2$; Right: zoom-in of surface level at $t = 2$.

Dam break over a plane

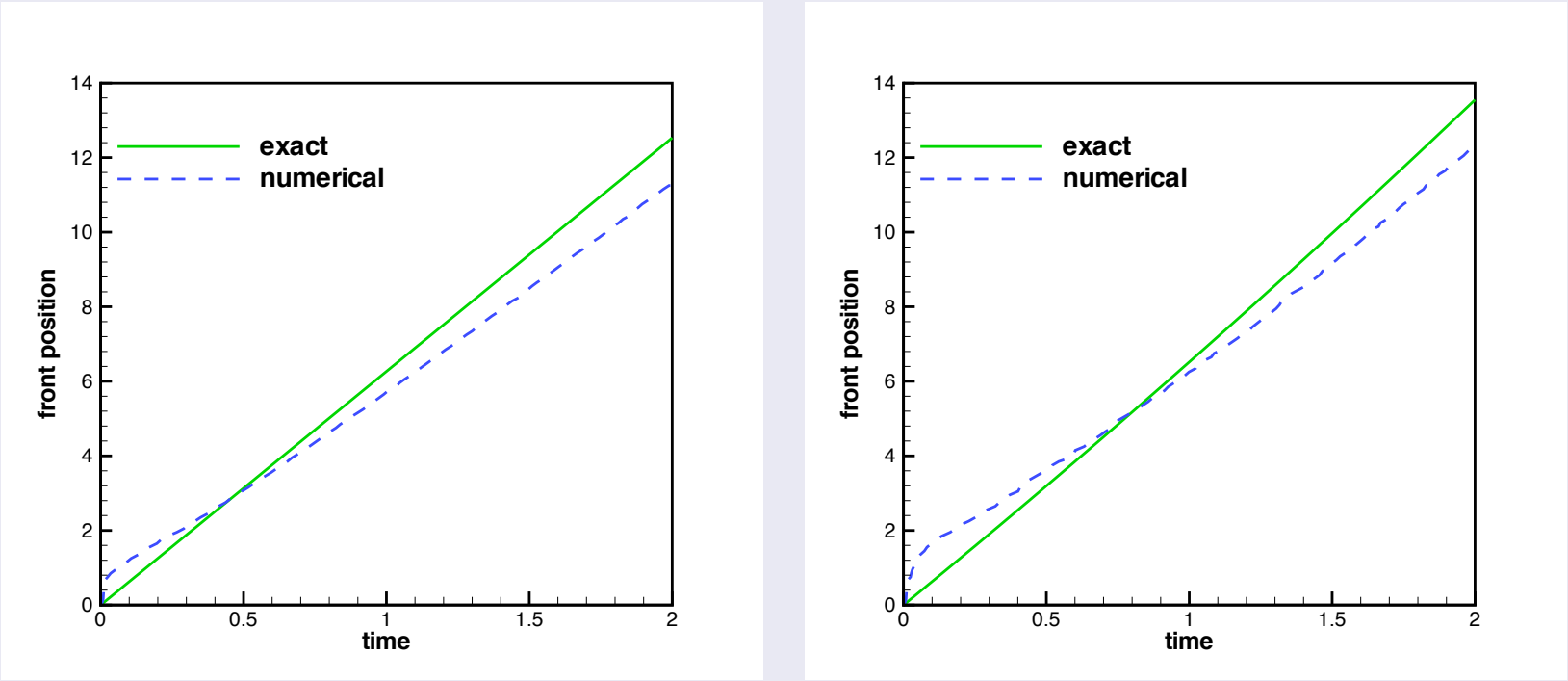

Figure: Time evolution of wet/dry front location. Left: flat bottom with $\alpha = 0$; Right: bottom with decreasing depth $\alpha = -\pi/60$.

Drain on a non-flat bottom

- In the computational domain $[0, 25]$,

$$b(x) = \begin{cases} 0.2 - 0.05(x - 10)^2 & \text{if } 8 \leq x \leq 12, \\ 0 & \text{otherwise.} \end{cases}$$

- The initial data is a still flat water

$$h(x, 0) = 0.5 - b(x), \qquad hu(x, 0) = 0.$$

- The left boundary condition is a free condition on h and zero on hu. The right boundary condition is an outlet condition on a dry bed.
- 250 uniform cells are used in the computation.

Drain on a non-flat bottom

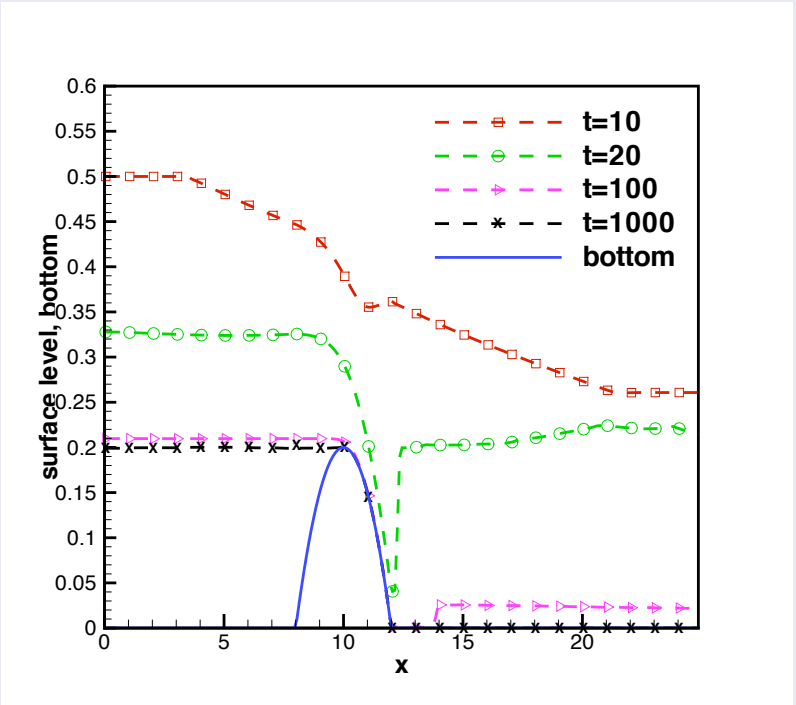

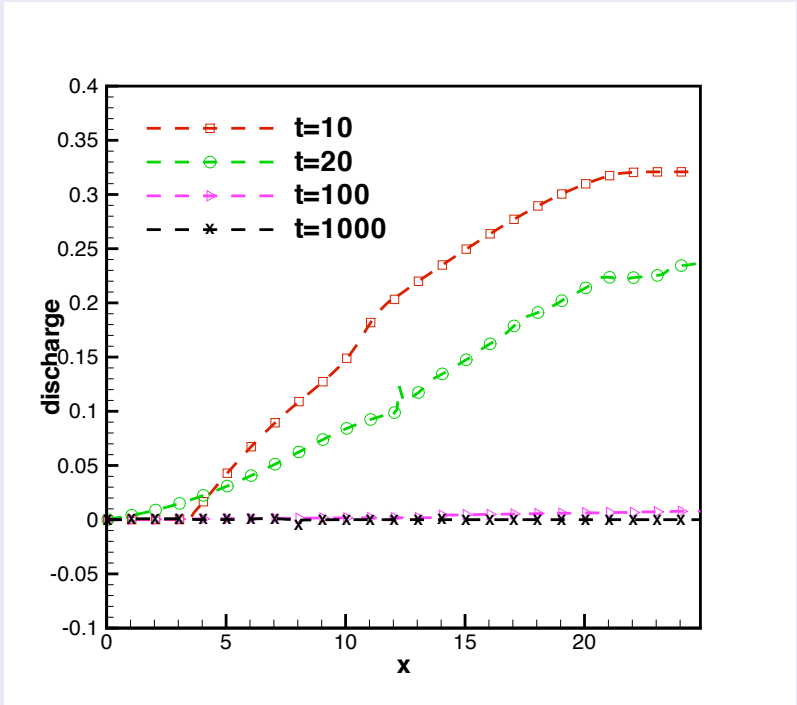

Figure: Drain on a non-flat bottom. Left: surface level at different time; Right: discharge at different time.

Vacuum occurrence by a double rarefaction wave

- In the computational domain $[0, 25]$,

$$b(x) = \begin{cases} 1 & \text{if } 25/3 \leq x \leq 12.5, \\ 0 & \text{otherwise.} \end{cases}$$

- The initial data is

$$h(x, 0) = 10 - b(x), \qquad hu(x, 0) = \begin{cases} -350 & \text{if } x \leq 50/3, \\ 350 & \text{otherwise.} \end{cases}$$

- 250 uniform cells are used in the computation.

Vacuum occurrence by a double rarefaction wave

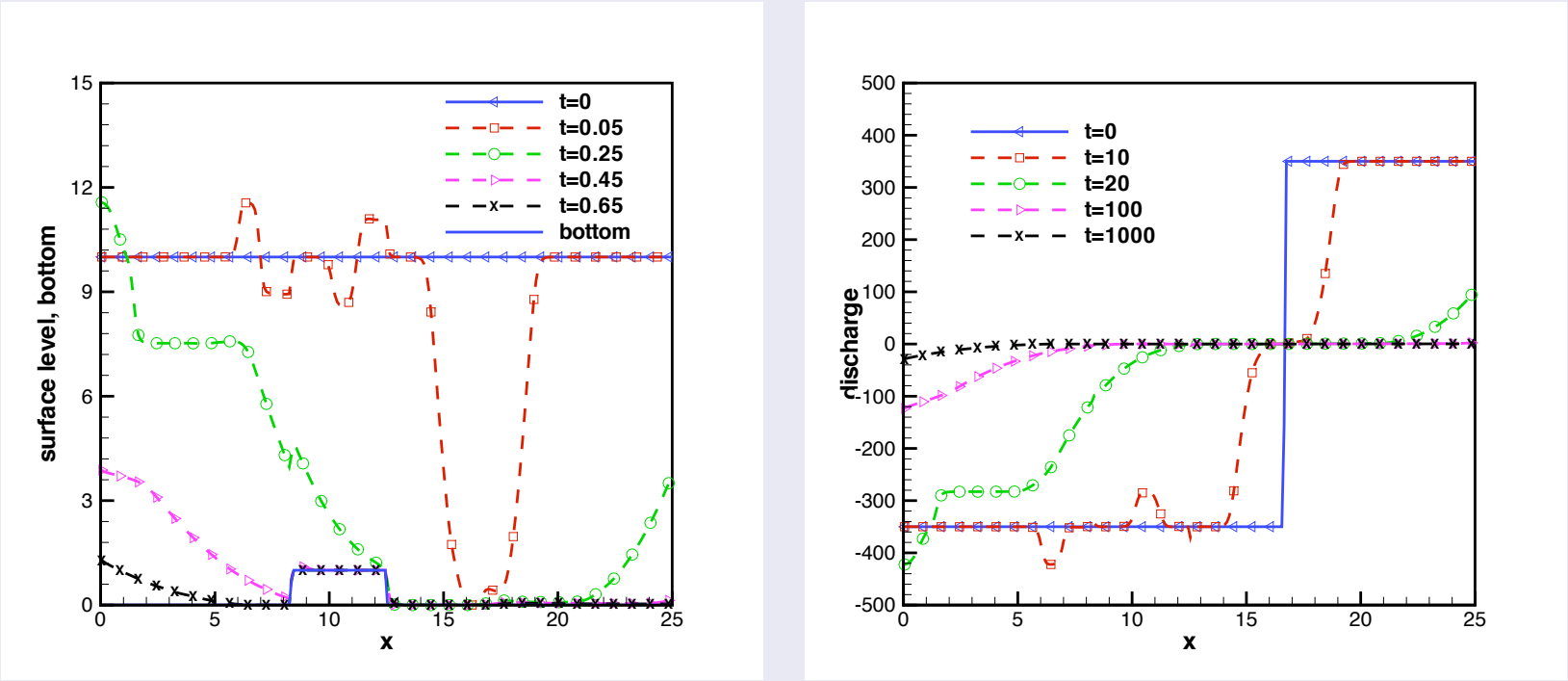

Figure: Vacuum occurrence by a double rarefaction wave over a step. Left: surface level at different time; Right: discharge at different time.

Two-dimensional oscillating lake

- A rectangular computational domain $[-2, 2] \times [-2, 2]$.
- The parabolic bottom topography takes the form

$$b(x, y) = h_0 \frac{x^2 + y^2}{a^2},$$

with constants h_0 and a to be specified later.

Two-dimensional oscillating lake

- The analytical solutions, are given by

$$
\begin{aligned}
h(x,y,t) &= \max\left(0, \frac{\sigma h_0}{a^2}(2x\cos(\omega t) + 2y\sin(\omega t) - \sigma + 0.1 - b(x,y))\right) \\
u(x,y,t) &= -\sigma\omega\sin(\omega t), \qquad v(x,y,t) = \sigma\omega\cos(\omega t),
\end{aligned}
$$

  periodic with the period $T = 2\pi/\omega$ and $\omega = \sqrt{2gh_0}/a$.

- Pick $a = 1$, $\sigma = 0.5$ and $h_0 = 0.1$ for our test case. The initial conditions are then defined by the above formula with $t = 0$.
- Stopping time $2T$ with 100×100 uniform cells

Two-dimensional oscillating lake

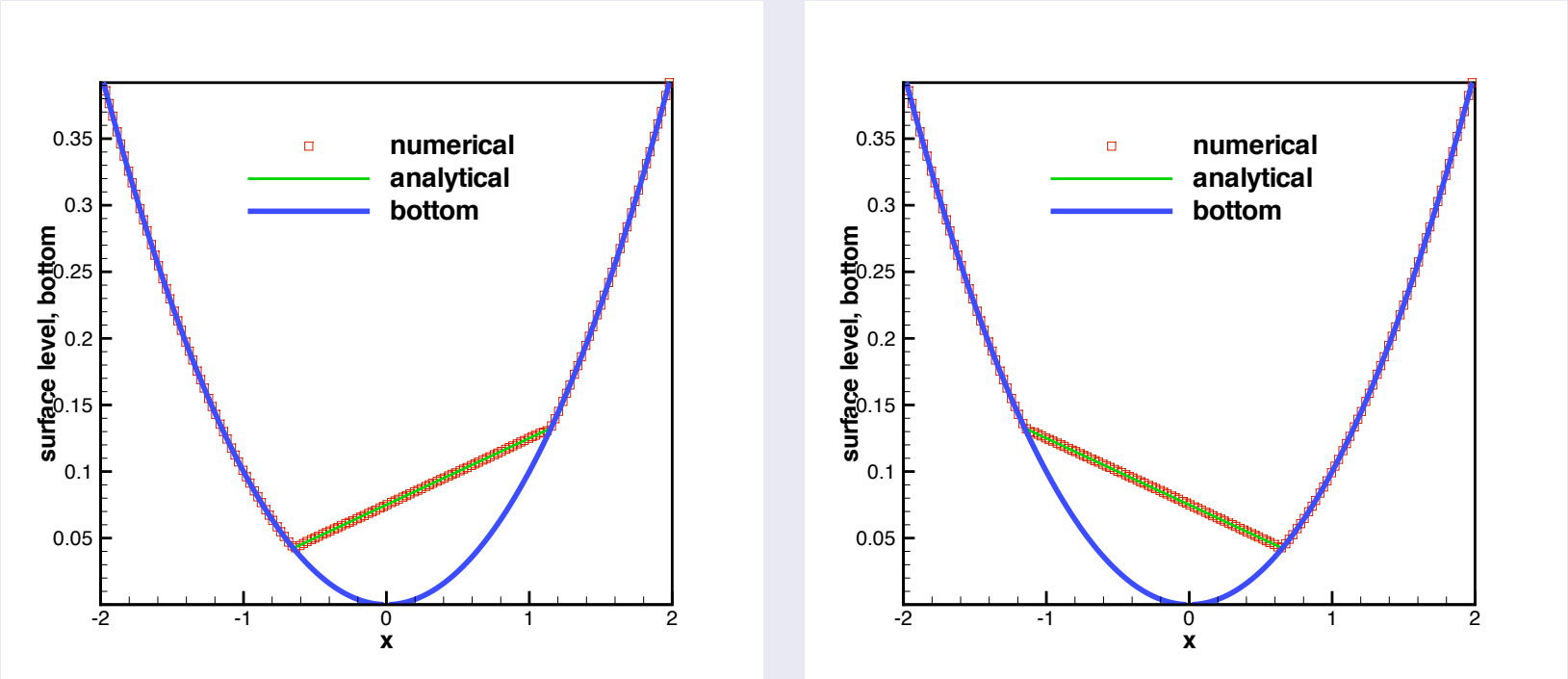

Figure: The 2D plot of the water surface level in the two-dimensional oscillating lake problem along the line $y = 0$ at different time. Left: $t = T/6$; Right: $t = T/3$.

Two-dimensional oscillating lake

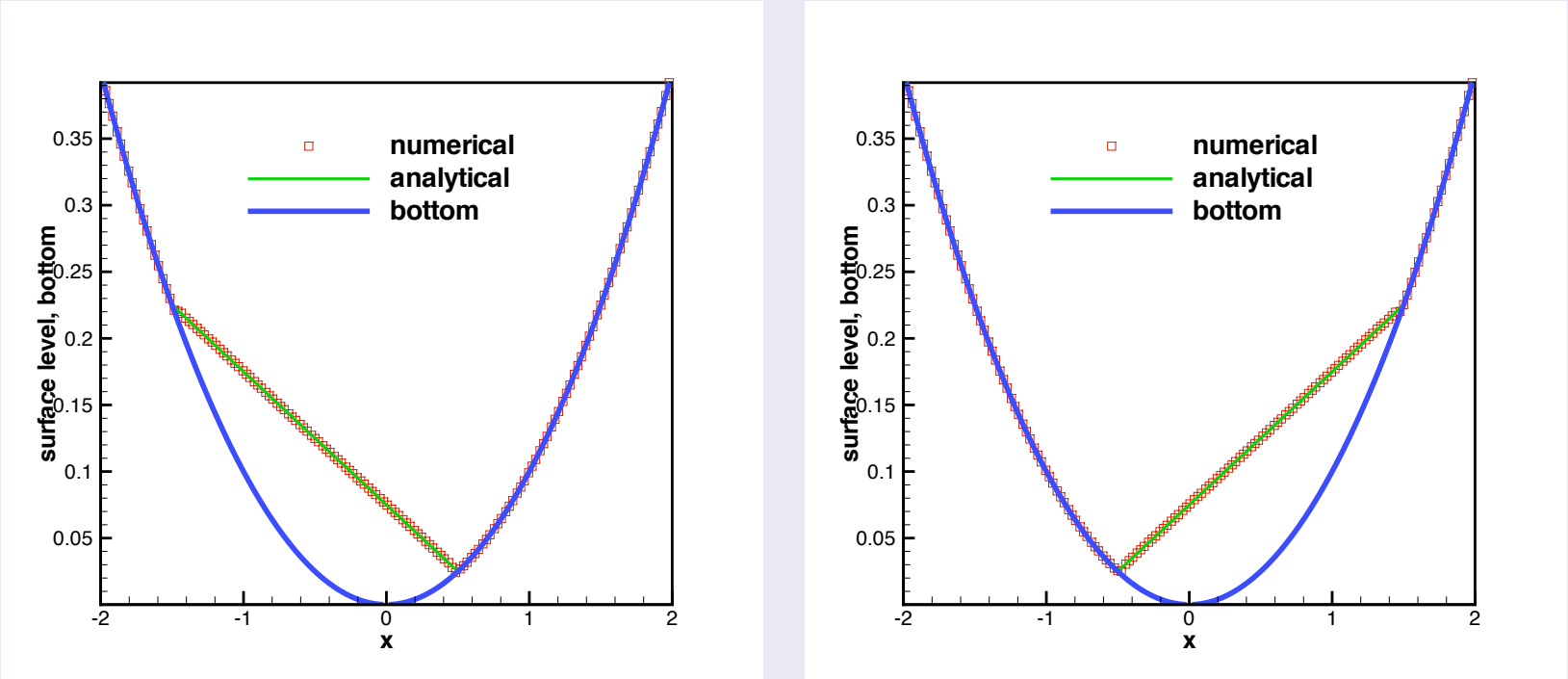

Figure: The 2D plot of the water surface level in the two-dimensional oscillating lake problem along the line $y = 0$ at different time. Left: $t = T/2$; Right: $t = 2T$.

Two-dimensional oscillating lake

(Loading movie...)

Summary and future work

- A simple positivity-preserving limiter based on high order DG/WENO methods for the shallow water equations, which can
  1. keep the water height non-negative,
  2. preserve the mass conservation,
  3. does not affect the high order accuracy for the general solutions.
- Two dimensional problems with triangular meshes, high order finite difference methods and multi-layer problems.

References

- Y. Xing and C.-W. Shu, **A new approach of high order well-balanced finite volume WENO schemes and discontinuous Galerkin methods for a class of hyperbolic systems with source terms**, *Communications in Computational Physics*, v1 (2006), pp. 100-134.
- Y. Xing, X. Zhang and C.-W. Shu, **Positivity-preserving high order well-balanced discontinuous Galerkin methods for the shallow water equations**, *Advances in Water Resources*, v33 (2010), pp.1476-1493.
- Y. Xing and C.-W. Shu, **High-order finite volume WENO schemes for the shallow water equations with dry states**, *Advances in Water Resources*, v34 (2011), pp.1026-1038.

Thank you!